PHYSICAL REVIEW A **73**, 021801(R) (2006)

Compact solid-state laser source for 1*S*-2*S* spectroscopy in atomic hydrogen

N. Kolachevsky,* J. Alnis,† S. D. Bergeson,‡ and T. W. Hänsch§
Max-Planck-Institut für Quantenoptik, Hans-Kopfermann-Strasse 1, 85748 Garching, Germany
(Received 18 November 2005; published 14 February 2006)

We demonstrate a compact solid-state laser source for high-resolution two-photon spectroscopy of the 1*S*-2*S* transition in atomic hydrogen. The source emits up to 20 mW at 243 nm and consists of a 972 nm diode laser, a tapered amplifier, and two doubling stages. The diode laser is actively stabilized to a high-finesse cavity. We compare the new source to the stable 486 nm dye laser used in previous experiments and record 1*S*-2*S* spectra using both systems. With the solid-state laser system, we demonstrate a resolution of the hydrogen spectrometer of 6×10^{11}, which is promising for a number of high-precision measurements in hydrogenlike systems.

DOI: 10.1103/PhysRevA.73.021801 PACS number(s): 42.55.Px, 42.62.Eh, 42.72.Bj, 32.30.Jc

Since the first experiments in the late 1970s [1], 1*S*-2*S* spectroscopy in atomic hydrogen and deuterium has provided essential data for fundamental physics. These include the determination of the Rydberg constant and tests of quantum electrodynamics theory [2,3], determination of nuclear properties of the proton and deuteron [3,4], spectroscopy of Bose-Einstein condensate in hydrogen [5], hyperfine structure measurements of the 2*S* state [6], and searching for the drift of the fine-structure constant [7].

In all of these experiments, the 2*S* state was excited by the second harmonic of a stabilized dye laser operating at 486 nm. The dye laser system originally developed in Garching has been repeatedly upgraded to meet the stringent requirements of high-resolution spectroscopic experiments. The uncertainty in recent 1*S*-2*S* frequency measurements in atomic hydrogen is 25 Hz ($\Delta f/f_0=1.0\times10^{-14}$, $f_0=2466$ THz) [7], an order of magnitude larger than the natural linewidth of 1.3 Hz. In addition to improving the accuracy of these measurements, it would be helpful to reduce the size of the experiment. This is not only necessary for metrological applications such as creating a transportable optical frequency reference, but also for opening possibilities for completely new experiments to test some fundamental aspects of physics.

For example, a number of recently proposed experiments concern spectroscopy of exotic atomic systems which are not available in the laboratory. This will require a new laser system to be set up close to the place where the atomic sample is produced. Experiments to study the 1*S*-2*S* spectroscopy in antihydrogen are prepared by the collaborations ATHENA (ALPHA) [8] and ATRAP [9] at CERN. A comparison between hydrogen and antihydrogen spectra should provide one of the most stringent tests of the CPT theorem. A frequency measurement of the 1*S*-2*S* transition in tritium could provide new independent information on the triton charge radius and its polarizability [10]. In addition, there is an ongoing activity on optical spectroscopy of positronium and muonium [11–13].

In this paper, we report a compact, transportable laser system that is suitable for such experiments. In the future it can replace stable but rather bulky dye-laser systems [7].

The laser source is a frequency-quadrupled master-oscillator power-amplifier (MOPA) system [14] (see Fig. 1). It is similar to the laser source demonstrated in Ref. [15]. An antireflection coated laser diode operating at 972 nm is placed in an external Littrow cavity. The output is amplified using a tapered amplifier (TA), producing up to 650 mW at

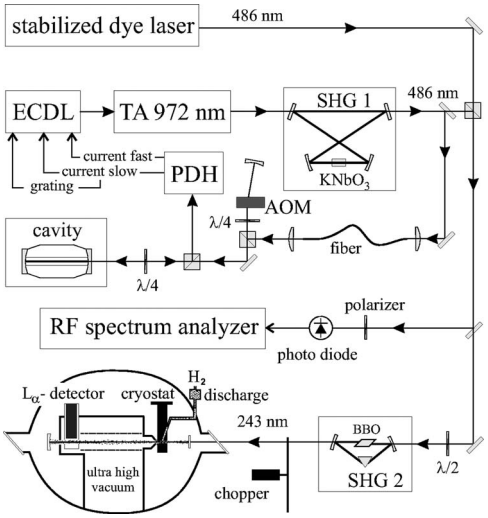

FIG. 1. A schematic diagram of the experimental setup. ECDL is the external cavity diode laser at 972 nm, TA is the tapered amplifier, SHG 1,2 are the second-harmonic-generation stages, PDH represents the Pound-Drever-Hall lock, and AOM is the acousto-optic modulator used for scanning the laser frequency. The output of the stabilized dye laser at 486 nm is superimposed with the output of the SHG 1 and is used both for the beat signal detection using a radiofrequency (RF) spectrum analyzer and for generation of 243 nm radiation. The hydrogen spectra are detected alternatively either using the dye laser or the solid-state system.

*Also at P.N. Lebedev Physics Institute, Leninsky prosp. 53, 119991 Moscow, Russia.

†Also at University of Latvia, 19 Rainis Blvd., LV-1586 Riga, Latvia.

‡Also at Brigham Young University, N283 ESC, Provo, UT 84602, USA.

§Also at Ludwig-Maximilians-University, Munich, Germany.

 ©2006 The American Physical Society

972 nm. This is coupled to the first doubling stage (SHG 1 in Fig. 1) consisting of a bow-tie build-up cavity around a $KNbO_3$ crystal. The crystal is used at normal incidence and is cut for phase matching at a temperature of 30 degrees. The cavity is locked to the laser using the Pound-Drever-Hall (PDH) technique [16], with a modulation frequency of 20 MHz. We have measured up to 210 mW at 486 nm. The astigmatism in this beam profile is corrected using a telescope with cylindrical lenses.

The light at 486 nm is split into two beams. About 10 mW is taken for frequency stabilization of the laser, while the remainder is sent to the second doubling stage (SHG 2 in Fig. 1) after proper mode-matching. The second frequency-doubling stage is a compact delta shape build-up cavity around a beta-barium borate (BBO) crystal [17]. After astigmatism compensation, we measure up to 20 mW at 243 nm in a near-Gaussian profile. The master oscillator, tapered amplifier, both doubling stages (SHG 1 and SHG 2), and some auxiliary optics are mounted on a single 60×120 cm^2 optical breadboard.

After a few months of operation, the output of the system decreased due to degradation of the TA beam profile. Laser powers were limited to 130 mW at 486 nm and 4.5 mW at 243 nm. Measurements reported in this paper were performed at this power level, which was enough to detect the $1S$-$2S$ transition. The TA has since been replaced, and the system has recovered the original specifications.

The laser is actively stabilized to a high-finesse cavity at 486 nm [18]. Cavity mirrors are optically contacted to a spacer produced from ultralow expansion (ULE) glass. The finesse of the cavity is 75 000, and the transmission peak is about 15 kHz full width at half-maximum (FWHM). The cavity rests on a ceramic support in a small vacuum chamber and can be fixed for transportation. The chamber is surrounded by single-stage temperature stabilization system and is placed in a $60\times60\times60$ cm^3 isolating box.

The ULE cavity is placed on a separate optical table. The 486 nm light from SHG 1 is delivered to the cavity by an optical fiber. To compensate for the frequency noise introduced by the fiber, a standard fiber noise compensation scheme is implemented (see, e.g., [19]). The laser frequency is stabilized to the cavity by a PDH lock at 11 MHz. The laser frequency can be shifted in respect to the frequency of the cavity mode using a double-pass acousto-optical modulator. The fact that we use the second harmonic for generating the PDH error signal does not change the phase characteristics of the lock since the transmission bandwidth of the SHG 1 is much broader than the bandwidth of the laser frequency noise.

The error signal is split into three channels. Fast current feedback is sent directly to the laser diode. Slow feedback is sent to the modulation input of the current controller. The low-frequency drift of the laser cavity is also compensated, using slow feedback to the grating. This feedback configuration is similar to that used in Refs. [20] and [21]. The amplitude of the closed-loop error signal measured in 50 kHz bandwidth corresponds to frequency noise on the level of 100 Hz at 486 nm. This value leaves a large room for improvement, but given the current level of acoustical vibrations of the transportable cavity, it is satisfactory.

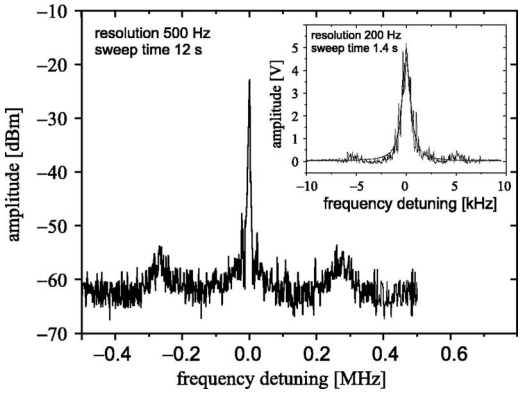

FIG. 2. Power spectrum of the beat note at 486 nm between the second harmonic of the diode laser and the dye laser in a logarithmic scale. Inset: The zoomed central part of the spectrum plotted on a linear scale. The dashed line shows a Lorentzinan fit with a 1 kHz FWHM.

The power spectrum of the diode laser is studied with the help of the independent stabilized dye laser used for the previous measurements [7]. The dye laser is locked to a nontransportable high-finesse ULE cavity which has significantly better acoustic isolation and temperature control compared to the cavity used for the diode laser stabilization. The typical frequency drift of the stabilized dye laser is on the level of about 0.2 Hz/s and its spectral linewidth $\Delta\nu_{\mathrm{dye}}$ is characterized as 60 Hz at 486 nm [22]. The power spectrum of the beat note between the two laser systems is presented in Fig. 2. The spectrum is defined by characteristics of the diode laser system, since on the given scale the dye laser possesses a negligible spectral linewidth and frequency drift and is essentially free of sidebands.

One can observe broad sidebands originating from the fast current feedback of the diode laser. The amplitude of the sidebands is sensitive to the strength of the feedback: with stronger feedback, more laser power is pushed into the sidebands. The central peak of the spectrum has a width of $\Delta\nu_{\mathrm{diode}}=1.0$ kHz FWHM at 486 nm. This mainly stems from acoustic vibrations of the transportable cavity to which the diode laser is locked.

The frequency drift of the diode laser can also be characterized using beat-note measurements. It is approximately 10 Hz/s at 486 nm, more then ten times higher than the frequency drift of the nontransportable cavity. Once again, this difference is attributable mainly to the optical cavity to which the diode laser is locked. The transportable cavity uses a simpler temperature controller and has greater thermal coupling to its ceramic support.

We tested the new diode laser source using the hydrogen spectrometer [7,22] depicted schematically in Fig. 1. The 243 nm radiation is coupled to a linear enhancement cavity, where the excitation of the hydrogen beam takes place. The flow of atomic hydrogen produced in a radio-frequency gas discharge is cooled to 5 K by a flow-through cryostat. Due to small apertures, only atoms flying close to the cavity axis can enter the detection region where the $2S$ atoms are quenched in a small electric field of a few volts per centimeter and emit Lyman-α photons. The excitation light is periodically

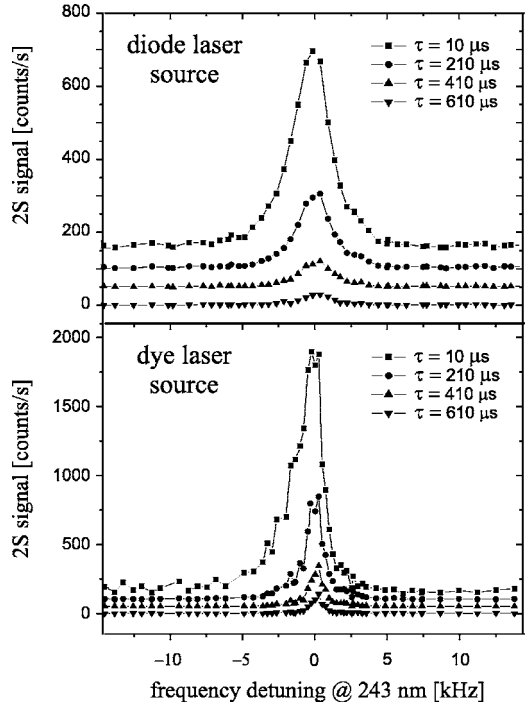

FIG. 3. Top: 1*S*-2*S* time-resolved spectra recorded with the diode laser source. The power of 243 nm radiation coupled to the enhancement cavity equals 2.6 mW. Bottom: 1*S*-2*S* spectra recorded with the dye laser source at the power of 2.2 mW. In each case, two spectra recorded in two different scan directions are averaged and the drift of the corresponding reference cavity is compensated. The plots corresponding to different delays are vertically shifted by 50, 100, and 150 counts.

blocked by a chopper operating at 160 Hz, and the L_α -photons are counted in a time-resolved way only in the dark part of a cycle. The delay τ between blocking the 243 nm radiation and the start of photon counting sets the upper limit for the atomic velocity of $v < l/\tau$, where l is the distance between nozzle and detector. The delay of $\tau = 1$ ms corresponds to the cutoff velocity of 130 m/s. With the help of a multichannel scaler, we count all photons and sort them into 12 adjacent time bins. For each laser detuning, the photons are accumulated during1 s. From each scan of the laser frequency over the hydrogen 1*S*-2*S* resonance, we therefore get up to 12 spectra measured with different delays. This detection scheme allows for evaluation of the second-order Doppler effect and reduces the background level that is due to scattered 243 nm radiation. The second-order Doppler shift can be corrected by use of a theoretical model which fits all the delayed spectra of one scan simultaneously [23].

A time-resolved spectrum of the 1*S*-2*S* transition excited using the new laser system is presented in Fig. 3 (top) for four different delays τ, where the photon count rate is plotted versus frequency detuning at 243 nm. The spectral linewidth of the transition $\Delta f_{\text{diode}}^{1S\text{-}2S}$ equals 2.8(1) kHz FWHM for $\tau = 10$ μs and reduces to 2.2(1) kHz for $\tau = 610$ μs. Besides the contribution of the finite linewidth of the excitation radiation, the 1*S*-2*S* transition linewidth is defined by time-of-flight broadening, power broadening, ionization broadening, and the second-order Doppler effect. The delayed detection significantly reduces the time-of-flight broadening and the second-order Doppler effect due to the velocity selection [23]. A detailed discussion of the linewidth is complicated by the fact that the population of the 2*S* state never reaches the steady state and the detection occurs in the transient regime [24]. The listed contributions are analyzed in detail elsewhere [24,25]. To analyze the spectrum in our particular case, we compare it to the calculated line shape using a Monte-Carlo approach for infinitely narrow excitation spectrum [25]. For the delay $\tau = 610$ μs, the simulated line has a FWHM at 243 nm of $\Delta f_{\text{theor}}(610\ \mu\text{s}) = 0.62$ kHz when 2.6 mW of 243 nm radiation coupled to the enhancement cavity.

Assuming Lorentzian profiles, one can write the following approximate relation:

$$\Delta f_{\text{diode}}^{1S\text{-}2S}(\tau) \simeq \Delta f_{\text{theor}}(\tau) + 2\,\Delta\nu_{\text{diode}}, \tag{1}$$

where $\Delta\nu_{\text{diode}} = 1.0$ kHz is the measured spectral width of the diode laser system at 486 nm. Factor 2 results from the frequency doubling in the SHG 2. In this particular case, the linewidth of the 1*S*-2*S* transition for longer delay times is mainly defined by the spectral linewidth of the excitation radiation. The spectral resolution of the spectrometer $f_0/\Delta f_{\text{diode}}^{1S\text{-}2S}(610\ \mu\text{s})$ equals 6×10^{11}.

To compare the diode laser source with the dye laser, we also performed a set of measurements with the dye laser coupled to the same doubling stage as depicted in Fig. 1. A 1*S*-2*S* spectrum recorded using the dye laser at a similar excitation power level is shown in Fig. 3 (bottom). The recorded lines are considerably narrower compared to the case of the diode laser. The line-shape asymmetry resulting from the second-order Doppler effect is clearly visible for short delays. Fast velocity classes efficiently contribute to the red side of the 1*S*-2*S* line and result in a broad wing of a few kHz wide. In turn, slow atoms from Maxwellian distribution contribute to the steep blue wing of the spectral line. The magnitude of the line shift is on the order of 1 kHz for $\tau = 10$ μs and reduces to about 100 Hz for $\tau = 610$ μs. By higher delays, the 1*S*-2*S* spectra become more symmetrical and approach the position of the unperturbed resonance. The amplitude noise partly results from the intensity fluctuations of the dye laser. The widths of the delayed spectra are close to the calculated ones: for example, $\Delta f_{\text{dye}}^{1S\text{-}2S}(610\ \mu\text{s}) = 0.75(5)$ kHz at 243 nm.

The 2*S* count rate in the line maximum recorded using the diode laser is approximately three times lower than using the dye laser. However, the power-normalized integrated signal from the diode laser system is $40 \pm 10\%$ of that from the dye laser system for all delays. This suggests that a significant fraction of the diode laser power lies outside of the 1 kHz Lorentian linewidth. This is not surprising, given the sideband amplitude measured in Fig. 2. The relative integrated line strength accurately reflects the excitation efficiency because we are in the limit $\Delta\nu_{\text{diode}} \gg \Delta f_{\text{theor}} \gg \Delta\nu_{\text{dye}}$.

It should be possible to narrow the spectrum of the diode laser using a two-stage, two-cavity lock scheme. Our diode laser is stabilized to a high-finesse cavity, and has a spectral width of approximately 1 kHz at 486 nm. This residual

width could be removed relative to a second cavity using an AOM. It is not enough simply to increase the feedback loop gain in the present setup. Increasing the gain only produces larger sidebands in the beat signal spectrum (see Fig. 2) and a subsequent loss of 2*S* excitation efficiency.

In summary, a high-power narrow-bandwidth diode laser source is reported that is capable of driving the 1*S*-2*S* two-photon transition in atomic hydrogen with a high signal-to-noise ratio. The spectral width of the laser is 2 kHz at 243 nm, limited mainly by the characteristics of the small, transportable optical cavity. One possible way to increase the short-term frequency stability of the optical cavity is to implement the new concept of vertically suspended cavities [26]. The proper choice of ULE zero-expansion point for the spacer would improve the long-term frequency stability of the diode laser source while keeping the whole system compact and transportable. This laser system is a promising source for spectroscopy of exotic hydrogenlike systems such as antihydrogen, tritium, positronium, and muonium.

N.K. acknowledges the support of DFG (Grant No. 436RUS113/769/0-1) and RFBR (Grants No. 03-02-04029 and No. 04-0217443). N.K. and S.D.B. acknowledge the support of the Alexander von Humboldt Foundation.

[1] T. W. Hänsch, *Laser Spectroscopy III*, Springer Series in Optical Sciences Vol. 7, edited by J. L. Hall and J. L. Carlsten (Springer, Berlin/New York, 1977). p. 149.
[2] F. Biraben, *et al.*, in *The Hydrogen Atom. Precision Physics of Simple Atomic Systems*, edited by S. G. Karshenboim, F. S. Pavone, G. F. Bassani, M. Inguscio, and T. W. Hänsch, (Springer, Berlin, 2001). p. 18.
[3] Th. Udem, A. Huber, B. Gross, J. Reichert, M. Prevedelli, M. Weitz, and T. W. Hänsch, Phys. Rev. Lett. **79**, 2646 (1997).
[4] A. Huber *et al.*, Phys. Rev. Lett. **80**, 468 (1998).
[5] T. C. Killian *et al.*, Phys. Rev. Lett. **81**, 3807 (1998).
[6] N. Kolachevsky, M. Fischer, S. G. Karshenboim, and T. W. Hänsch, Phys. Rev. Lett. **92**, 033003 (2004).
[7] M. Fischer *et al.*, Phys. Rev. Lett. **92**, 230802 (2004).
[8] M. Amoretti *et al.*, Nature (London) **419**, 456 (2002).
[9] G. Gabrielse *et al.*, Phys. Rev. Lett. **89**, 213401 (2002).
[10] B. F. Gibson, Lect. Notes Phys. **260**, 511 (1986).
[11] R. Ley, Appl. Surf. Sci. **194**, 301 (2002).
[12] K. Jungmann *et al.*, Z. Phys. D: At., Mol. Clusters **21**, 241 (1991).
[13] D. Habs (private communications).
[14] The frequency-doubled MOPA is a modified commercial system from Toptica Photonics AG, model TA-SHG 110-980.
[15] C. Zimmermann, V. Vuletic, A. Hemmerich, and T. W. Hänsch, Appl. Phys. Lett. **66**, 2318 (1995).
[16] R. W. P. Drever *et al.*, Appl. Phys. B **31**, 97 (1983).
[17] SHG 2 is from Spectra-Physics Inc., model WT477-500.
[18] C. Niessl, Diploma thesis, Ludwig-Maximilians University Munich, Germany.
[19] C. Daussy *et al.*, Phys. Rev. Lett. **94**, 203904 (2005).
[20] A. Schoof, J. Grünert, S. Ritter, and A. Hemmerich, Opt. Lett. **26**, 1562 (2001).
[21] G. Biandhini *et al.*, Appl. Phys. B **66**, 407 (1998).
[22] M. Fischer *et al.*, in *Astrophysics, Clocks and Fundamental Constants*, Lecture Notes in Physics Vol. 648, edited by S. G. Karshenboim and E. Peik (Springer, Berlin, 2004). p. 209.
[23] A. Huber, B. Gross, M. Weitz, and T. W. Hänsch, Phys. Rev. A **59**, 1844 (1999).
[24] M. Haas *et al.* (unpublished).
[25] N. Kolachevsky *et al.* (unpublished).
[26] M. Notcutt, L.-S. Ma, J. Ye, and J. L. Hall, Opt. Lett. **30**, 1815 (2005).